UNIVERSITAT POLITÈCNICA DE VALÈNCIA
DEPARTMENT OF AGROFORESTRY ECOSYSTEMS

Master's Degree in Plant Health in Sustainable Cropping Systems

Master's Thesis

Development of Multispectral Indices for Organic Fertilization Monitoring in Tomato Plants at Early Stages

Matheus Cardim Ferreira Lima

Tutor: Dr. Josep Armengol Fortí
External Tutor: Dr. Constantino Valero

September, 2019

Co-funded by the Erasmus+ Programme of the European Union

Desarrollo de índices multiespectrales para el monitoreo de la fertilización orgánica de plantas de tomate en estadios iniciales.

Resumen

Se ha desarrollado un sistema de monitoreo de cultivos para supervisar el estado nutricional de las plantas de tomate en las primeras etapas de desarrollo. Se utilizó un enfoque automático y no destructivo para analizar las plantas de tomate con diferentes niveles de fertilizante orgánico soluble en agua (3 + 5 NK) y humus de lombriz. El sistema de evaluación estaba compuesto por una cámara multiespectral con cinco lentes: verde (550nm), rojo (660nm), borde rojo (735nm), infrarrojo cercano (790nm) + 16MP RGB y un sistema de procesamiento de imágenes computacional. El fertilizante soluble se aplicó semanalmente en cuatro tratamientos diferentes: (T0: 0 ml, T1: 6.25 ml, T2: 12.5 ml y T3: 25 ml) y el vermicompost se añadió en la primera (T0: 0 ml; ml, T2: 150 ml, T3: 300 ml) y en la quinta semana (T0: 0 ml, T1: 237.5 ml, T2: 475 ml, T3: 950 ml). El ensayo se realizó en invernadero y se tomaron 192 imágenes con cada lente. Se desarrolló un algoritmo de segmentación y múltiples índices de vegetación fueron calculados: Índice de Vegetación de Diferencia Normalizada (NDVI), Índice de Vegetación de Diferencia Normalizada Verde (GNDVI), Índice de Vegetación de Diferencia Normalizada de Borde Rojo (RENDVI), Índice de Vegetación No Lineal (NLI), Índice de Vegetación Ajustado y Optimizado para el Suelo (OSAVI), Índice de Vegetación de Proporción Verde (GRVI), Proporción Simple (SR), Proporción Simple Modificada (MSR), Índice de Pigmento Intensivo de Estructura 2 (SPI2) e Índice de Clorofila de la Hoja (LCI). Adicionalmente al cálculo de índices, se obtuvieron múltiples características morfológicas a través del procesamiento de imágenes y los resultados se compararon entre los tratamientos utilizando la prueba HSD de Tukey con un 1% de probabilidad. Las características morfológicas tales como: Área, Área rellena, Área convexa, Perímetro, Longitud del eje mayor, Longitud del eje menor y Diámetro Equivalente se revelaron más útiles para distinguir entre el control y las plantas fertilizadas orgánicamente que los índices de vegetación. El sistema fue desarrollado para ser ensamblado en una plataforma robótica de fertilización orgánica de precisión.

Palabras clave: imagen multiespectral, visión computacional, agricultura de precisión, índices de vegetación.

Development of multispectral indices for organic fertilization monitoring of tomato plants at early stages

Abstract

A crop monitoring system was developed for the supervision of organic fertilization status on tomato plants at early stages. An automatic and nondestructive approach was used to analyze tomato plants with different levels of water-soluble organic fertilizer (3+5 NK) and vermicompost. The evaluation system was composed by a multispectral camera with five lenses: green (550nm), red (660nm), red edge (735nm), near-infrared (790nm) + 16MP RGB and a computational image processing system. The water-soluble fertilizer was applied weekly in four different treatments: (T0: 0 ml, T1: 6.25 ml, T2: 12.5 ml and T3: 25 ml) and the vermicompost was added in the 1st (T0: 0ml; T1: 75 ml; T2:150ml; T3: 300 ml) and in the 5th week (T0: 0ml; T1: 237,5 ml; T2:475ml; T3: 950 ml). The trial was conducted in a greenhouse and 192 images were taken with each lens. A plant segmentation algorithm was developed and several vegetation indices were calculated: Normalized Difference Vegetation Index (NDVI), Green Normalized Difference Vegetation Index (GNDVI), Red-Edge Normalized Difference Vegetation Index (RENDVI), Nonlinear Vegetation Index (NLI), Optimized Soil Adjusted Vegetation Index (OSAVI), Green Ratio Vegetation Index (GRVI), Simple Ratio (SR), Modified Simple Ratio (MSR), Structure Intensive Pigment Index 2 (SPI2) and Leaf Chlorophyll Index (LCI). On top of calculating the indices, multiple morphological features were obtained through image processing techniques, and the results were compared between treatments using Tukey's HSD test with 1% of probability. The morphological features such as Area, Filled Area, Convex Area, Perimeter, Major Axis Length, Minor Axis Length and Equivalent Diameter revealed to be more feasible to distinguish between the control and the organic fertilized plants than the vegetation indices. The system was developed in order to be assembled in a precision organic fertilization robotic platform.

Keywords: multispectral image, computer vision, precision agriculture, vegetation indices

Author of the Master Thesis: Matheus Cardim Ferreira Lima

Academic Tutor: Dr. Josep Armengol Fortí

External Tutor: Dr. Constantino Valero Ubierna

Acknowledgements

I would like to express my sincere gratitude to my supervisors Dr. Josep Armengol Fortí, and Dr. Constantino Valero for providing their invaluable guidance, comments and suggestions through the course of the project. I would also thank Anne Krus for the assistance with the code optimization and the Centre of Automatics and Robotics of the CSIC for providing the Parrot Sequoia Camera. I express my cordial gratitude to all my Plant Health colleagues, especially to Clara Bazzo, Maria Elisa Damascena, Murilo Sandroni and Franscesca Laurini, for all the nights of study and support during these years. I am also pleased to express my sincere gratitude to all my family and Hanwool Sung for the unconditional support, and to the European Commission for making this Master happened.

This master's thesis has been developed as a result of a mobility stay funded by the Erasmus+ - KA1 Erasmus Mundus Joint Master Degrees Programme of the European Commission under the PLANT HEALTH Project.

Contents

List of Tables

List of Figures

Introduction

Environmental protection allied with health concerns are increasingly important trends in the consumers' behaviour and leading to the development of green products and organic markets (Hidalgo-Baz *et al.* 2017).

These markets are experiencing exponential growth in the last years, especially the organic markets that address multiple consumer concerns relating to health, food safety and environmental conservation (Pino *et al.*, 2012).

On a global level, the organic agricultural land area increased by 6.5 million hectares compared with 2014. The vegetable organic production, for example, increased from 299.301 ha in 2014 to 675.980 ha in 2017 (IFOAM, 2019). Tomatoes command a larger share of fresh vegetables market worldwide, the organic tomato sales continue to rise, increasing the market value in 20% between 2015 and 2016 (IndexBox, 2017).

The economical healthy growth of the sector is expected to continue; however, some challenges are presented in the horizon regarding the concentration of the demand, the rising number of standards, supply shortfalls among other factors (Willer *et al.,* 2019)

Tomatoes are one of the vegetable crops with higher demand for fertilization, with recommended doses close to 400kg.ha-1 depending on soil type (Ribeiro *et al.,* 1999).

Deficient use of organic fertilization can cause “abiotic diseases” on plants, decrease the suppressive effect of the soil and the readiness of plants to defend themselves against attacks of plant pathogens (Agrios, 2005; Kenelly *et al.,* 2012). The nutrient deficiency affects the plant growth, with consequences in the production and the profitability of the organic field; on the other hand, indiscriminate use of manure and soluble fertilizers prolong the vegetative state of the plant with abundance of young tissue, making the plants more susceptible for plant pathogens attacks and vulnerable for a longer time (Agrios, 2005; Brown and Ogle, 1997); besides that a considerable amount of the fertilizers cannot be totally absorbed by the plants.

These compounds can also run off into waterways, leached into groundwater or lost in gaseous form. The leachate liquid derived from the organic fertilizer can cause pollution of groundwater producing toxic algae blooms, accelerating eutrophication and reducing biodiversity (Wang *et al.* 2019).

These damaging effects are causing changes in the legislation in many regions – including Europe – in order to reduce or minimize the use of organic and mineral compounds such as manure and copper (Ghorbani *et al.,* 2010; IFOAM, 2019).

Meta-analysis studies indicate that the optimization of the use of nitrogen fertilization in tomatoes can decrease costs and environmental impact maintaining the same yield levels (Du *et al.,* 2018).

Focusing on that, the European commission fomented projects to study cost-efficiency technologies and bring innovations to reduce the dependency of contentious inputs in the organic production systems. Projects such as RELACS and SUREVEG are examples of European efforts to understand the dynamics of organic systems in order to reduce the use of external inputs.

RELACS seeks to promote the development and adoption of environmentally safe and economically viable tools and technologies to reduce the use of external inputs in organic farming systems.

SUREVEG is funded by the Coordination of European Transnational Research in Organic Food and Farming Systems and seeks to develop and implement innovations for the intensive cropping systems using strip-cropping and fertility strategies. One of the research lines aims the development and test of smart technologies for the management of strip-cropping systems.

These smart technologies are focused on the use of precise fertilization methods to reduce the dependency of biopesticides and non-organic fertilizers, improve soil fertility in intensive vegetable cropping systems and therefore bring a positive impact on water quality and landscape biodiversity (Kristensen, 2019).

The field of precision fertilization aims to optimize the use of resources in time and space. Smart technologies were developed for monitoring the nutrient status of plants and control variable rate applications in broad, monocrop, and conventional fields (Stafford, 2019).

Initially these technologies were based on soil samples, yield mapping and automatic guidance (Chen *et al.* 2014). After that, the advances in sensor technology-enabled nondestructive optical approaches and the use of satellite and unmanned aerial vehicles images were added to the system (Candiago *et al.,* 2015). Nowadays new embedded devices have been implemented in order to analyze the nutrient status of the crop in real-time using high-resolution image sensors at plant level (Pallottino *et al.* 2019).

These sensors are based on multispectral images and use vegetation indices to obtain the best correlation with the nutrient status of the arable crops (Prey *et al.,* 2018; Kitíc *et al.*, 2019; Freidenreich *et al.,* 2019).

In real-time sprayer systems, these devices are embedded in conventional tractors and are connected to Global Navigation Satellite System (GNSS) and computer system that controls selectively foliar spray applications (Pedersen *et al.,* 2017).

Other systems based in real-time analysis were developed in order to deliver site-specific herbicide applications in arable crops. Besides the multispectral images and the vegetation indices, these systems use a bicameral system, binarization techniques and morphological algorithms to differentiate between the crop and spontaneous plant species (Gerhards, 2006; Christensen 2009; Ávila-Navarro *et al.,* 2019; Partel *et al*., 2019).

Both types of real-time precision spraying systems are commercially available or in process of being commercialized, and showed a positive reduction in the use of chemical compounds with a reduction of costs and with an increase in the yield levels (in the case of precision fertilization) compared to traditional sprayers (Pedersen *et al.,* 2017).

Image processing techniques with multispectral cameras from visible to near-infrared spectrum are also being used to provide non-destructive plant phenotype image datasets. These approaches allowed more precise and real-time, high throughput and high-resolution data for modelling and prediction of plant growth and morphological development in different conditions, with recent applications in plant health analysis (Ampatzidis *et al.,* 2017; Chawade *et al.,* 2019; Veys *et al.,* 2019).

More advanced prototypes were made in order to insert these types of sensors in autonomous vehicles. Several terrestrial robotic platforms were developed using multispectral cameras seeking for a more automatic, low-energy cost and accurate analysis of the crop parameters compared to conventional equipped tractors and unnamed aerial vehicles (Grimstad and From 2017; Shamshiri *et al.,* 2018; Pallottino *et al*., 2019).

Some of these autonomous agricultural devices were capable of identifying weeds and control them using low-dose spraying, mechanical control or thermal control (King, 2017). Other platforms can spray fertilizers in arable crops without the need for heavy tractors, reducing the compaction of the soil and the physical damage to the crops (Cavender-Bares and Bares*.,* 2019).

Most recently, modular agricultural robots were developed for mapping different aspects of the cereal plants in parcels of breeding trials, these machines can also control fungal pathogenic spore dispersion using guided UV light inside greenhouses (Grimstad and From 2017).

Besides the advances in the robotic agricultural platforms, most of them were developed for conventional orchards and arable crops, presenting a lack of technologies in the context of organic horticulture.

This work aims to acquire multispectral images of Tomato plants with different levels of organic fertilization and estimate the nutritional state of the plant in the early stages using multiple vegetation indices and morphological features by using computer vision techniques.

The obtained knowledge will be implemented into a robotic platform prototype used to monitor and apply organic fertilizers in real-time, in order to optimize the use of this components within the organic horticultural context.

Research Methodology

Location and Growing Conditions

The experiment was carried out on a greenhouse in order to obtain the different spectral responses of plants. The experimental area was located in Madrid, Spain (40°26'19.9"N 3°44'15.7"W). The tomato (Mina F1 cv.) seedlings were initially cultivated at 3-litre pots with a diameter of 15 centimeters, filled with a substrate mix of turf and coconut fiber. After 5 weeks the plants were transplanted to 8-litre pots.

Trial Design and Fertilization

The experiment was designed as randomized blocks, with four treatments and six repetitions. The fertilizations were carried out weekly using water-soluble organic fertilizer (3+5 NK) obtained from beet vinasse and phosphorite, and registered for use in organic production. The initial volume of the irrigation and fertilization was 300ml of solution. One week after transplant, plants were assigned to the different treatments according to the fertilizer label (T0: 0 ml, T1: 6.25 ml, T2: 12.5 ml and T3: 25ml). The plants also received two supplements of vermicomposting (T0: 0ml; T1: 75 ml; T2:150ml; T3: 300 ml) and another one after the second transplant (T0: 0ml; T1: 237,5 ml; T2:475ml; T3: 950 ml). Images of the plants were acquired with 7-days interval. The statistics were analyses were carried out through the ANOVA and Tukey's test at 99% of confidence for average comparisons. The images were processed through the software MatLab, using the image processing toolkit. The methodology was composed by the following steps: Image pre-processing, vegetation indices, plant extraction,

morphological analysis and statistical analysis. The statistical analysis was carried out using the statistical and machine learning toolbox present in the same software.

System Overview

The general system was composed of images acquired from the greenhouse experiment with different levels of fertilization, the computational processing system and the statistical analysis.

The evaluation system was composed by a Bracket Support Stands Clamp supporting the sensor and the power supply (battery). The platform has the possibility of height adjustment for the sensor. The distance between the sensor and the bottom of the pot was set at 0.7 m during the first 5 weeks and moved to 1.4m after the 5^{th} week (Figure 1).

The pots used in the early stages (until 5 weeks after transplant were of 3-litre with 15 cm of height and 15 cm of diameter, in the subsequent weeks the plants were transplanted to 8-litre pots both with a mixture of 50% of coconut fibre and 50% of turf.

The camera used for image acquisition was a multispectral camera (model Sequoia, Parrot Drones, 2017) which was originally designed for use in agricultural Unmanned Aerial Vehicles (UAV's). Its internal sensor is composed of four spectral bands which register the reflected light coming from the vegetation and can be used to distinguish plant vigour based on reflectance levels (Xue *et al.* 2019). These bands are: Green (550nm wavelength, 40nm bandwidth), Red (660nm wavelength, 40nm bandwidth), Red Edge (735nm wavelength, 10nm bandwidth) and Near Infrared (790nm wavelength, 40nm bandwidth). Additionally, a 16-megapixel RGB camera is also fitted into the commercial system.

The Sequoia Camera has also a sunshine sensor that is used to calibrate the images depending on the sunlight. This makes it possible to compare photos over time, despite variations in light during photo shoots. The sunshine sensor is attached on the upper part to the system, facing the sky and correcting the signal and it also contains a GPS/GNSS module, a magnetometer and inertial measurement system (Parrot Drones, 2017) (Figure 1).

The images were taken with and without a black background placed to help the segmentation. The developed algorithms showed different efficiency in segmentation with or without the background. The pots were tagged with a coloured stamp in order to take the images in the same position during the experiment. The sensor communicates

with a smartphone or computer via Wifi protocol (Figure 2) in order to store the acquired images.

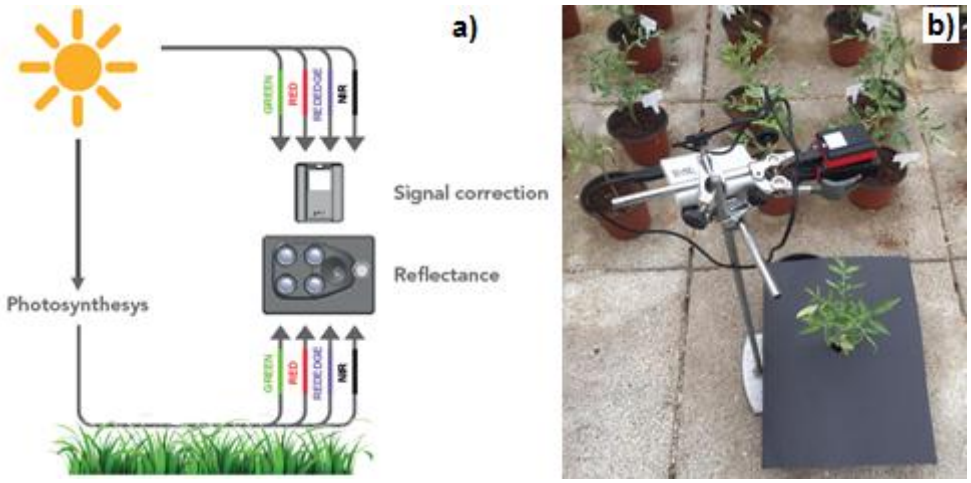

Figure 1 – Overview of the image acquisition system. a) Conceptual image acquisition scheme (Parrot Drones, 2017). b) Bracket support with camera and signal correction device measuring tomato plants in early stages.

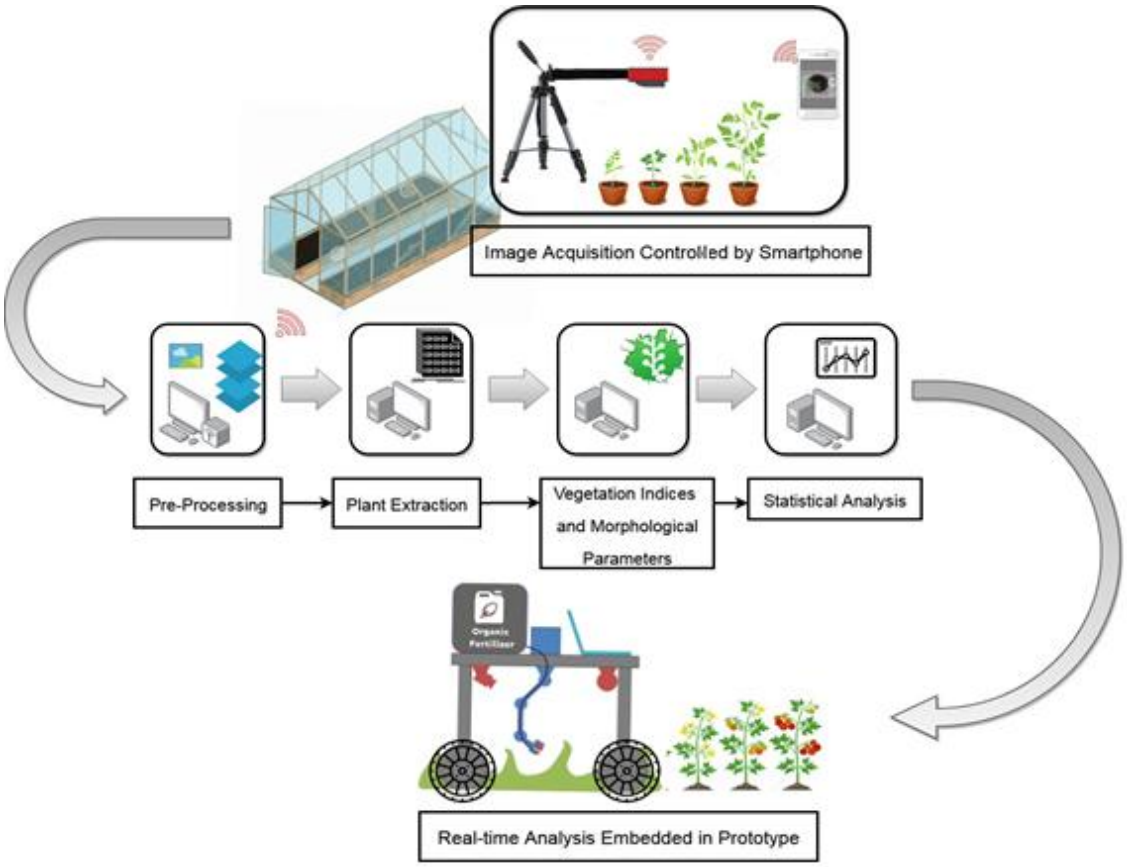

Figure 2 – Methodology implemented to develop a system for automatic fertilization in organic tomato plants at early stages.

Computational system for image analysis

The computational system used for the image analysis is composed of four major steps: pre-processing, calculation of vegetation indices, image segmentation, and morphological analysis.

1.1 Image Pre-Processing

The Sequoia sensor produces Tagged Image File Format (TIFF) images with a size of 1280 x 960 pixels. The camera was designed to take images from a minimum distance of 30 m to the target (Parrot Drones, 2017). When the images were taken with a shorter distance a displacement occurs between the 4-channel images due to an unexpected geometry between the sensors. In order to correct the displacement of the images, an algorithm that shifts an image by a specified number of pixels in either the *x*- or *y*-direction (or both) was used.

The parameters used to define the number of pixels and the direction that each image should be shifted were obtained using a sample image with a referential point and then applied subsequently to all collected data.

The red image was arbitrarily selected as the reference, and then the green, near-infrared (NIR) and red-edge images were shifted in order to be in the same position as the red image. The parameters used for the distances (0.7m – 1.3m) are shown in Table 1.

Table 1 – Shift factors (*x*- and *y*-direction) used for overlaying the different images using parrot sequoia in shorter distance of plant samples. (Red image used as reference).

Images	Shift Factor
Green	[50, 23]
Near Infrared	[41, -34]
Red Edge	[68, -11]

The central area of the images was defined as Area of Interest (AOI) and the consequent processes were used in this area in order to reduce the computational process and optimize the plant recognition and binarization. The images were clipped with AOI-*x*: 200:900 and AOI-*y* 200:1000, reducing the size of the image from 960 x 1280 to 700 x 800 squared pixels (Figure 3).

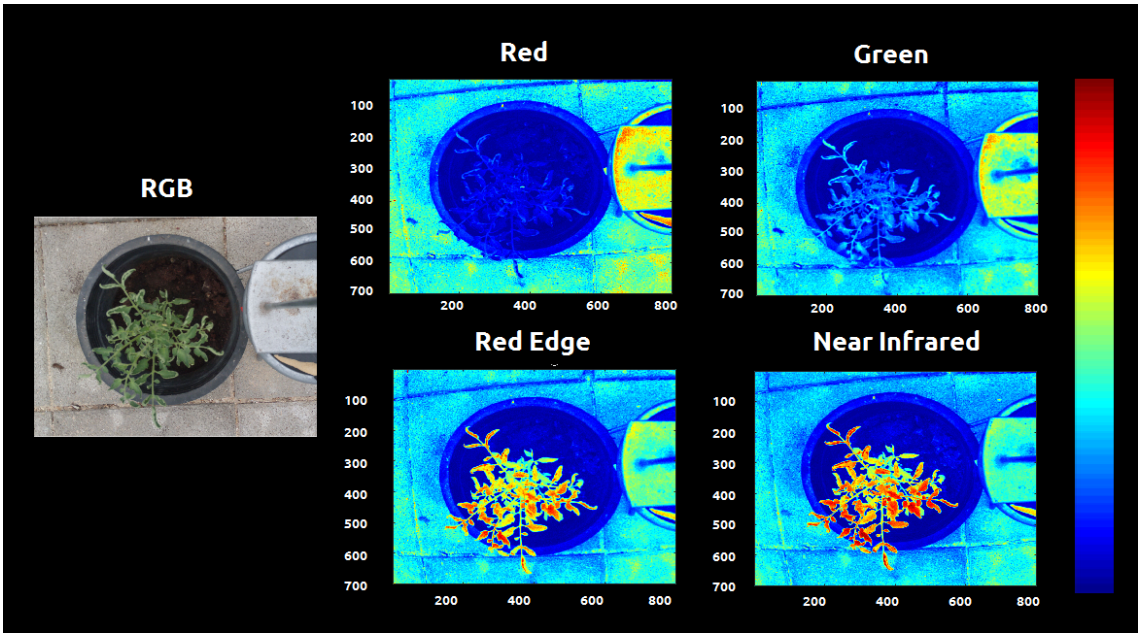

Figure 3 – Types of images produced by the sensor after shifting and clipping the area of interest (700 x 800 resolution). (Bluish colours indicate regions with lower levels of reflectance and reddish colours indicates regions with higher levels of reflectance).

1.2 **Vegetation Indices**

Obtained from multispectral images, Vegetation Indices (VIs) are quite simple and effective parameters for qualitative and quantitative evaluations of vegetation vigour, cover and growth dynamics among other applications. There is a vast implementation of these indices using different airborne and satellite platforms with recent advances using Unmanned Aerial Vehicles (UAV) and tractors. Due to the complexity of the instrumentation platforms, light spectra combinations and resolutions used, there is no unified mathematical expression that attends all applications of VIs (Xue and Su., 2017).

According to the same authors, customized algorithms have been studied for several applications combining visible light radiation, mainly the spectral region correspondent with the green region from vegetation, and nonvisible spectra in order to obtain proxy quantifications of the vegetation surface.

Therefore, for precise measurement applications, the VIs are optimized and usually constructed according to the specific application requirements, and a validation procedure is needed, along with customized methodologies.

Seeking for correlations between the fertilization status of the Tomato plants with the spectral response, eleven VIs presented in the literature were analyzed and tested. One of the vegetation indices were also used as a filter parameter for binarization of the plant leaves despite the background (image segmentation).

The VI's were chosen based on the literature and in the available bands present at the sensor. The list of indices, abbreviations, formula and traditional application of the VIs can be observed in Table 2. For use in this study, some closest Sequoia reflectance bands were substituted for the traditional narrowband wavelengths.

The images were converted from unit8 to double type in order to allow the pixels to admit decimal values and calculations. All the image processing analysis was performed in the Matlab software (2013b, The MathWorks Inc., Natick, MA, USA).

Table 2 – Vegetation Indices (VIs) used to create spectral profiles of the tomato plants from the multispectral data with formulae and traditional applications.

Index	Abbreviation	Formula	Application
Normalized Difference Vegetation Index	NDVI	$\frac{\rho\text{NIR} - \rho\text{RED}}{\rho\text{NIR} + \rho\text{RED}}$	Measuring green vegetation through normalized ration ranging from -1 to 1.
Green Normalized Difference Vegetation Index	GNDVI	$\frac{\rho\text{NIR} - \rho\text{GREEN}}{\rho\text{NIR} + \rho\text{GREEN}}$	Modification of NDVI, more sensitive to chlorophyll content.
Red-Edge Normalized Difference Vegetation Index	RENDVI	$\frac{\rho\text{NIR} - \rho\text{RedEdge}}{\rho\text{NIR} + \rho\text{RedEdge}}$	Modification of NDVI, using Red-Edge information related to plant health.
Nonlinear Vegetation Index	NLI	$\frac{\rho\text{NIR}^2 - \rho\text{RED}}{\rho\text{NIR}^2 + \rho\text{RedEdge}}$	Modification of NDVI used to emphasize linear relations with vegetation parameters.
Optimized Soil Adjusted Vegetation Index	OSAVI	$1.5 * \frac{\rho\text{NIR} - \rho\text{RED}}{\rho\text{NIR} + \rho\text{RED} + 0.16}$	Variation of NDVI in order to reduce the soil effect
Green Ratio Vegetation Index	GRVI	$\frac{\rho\text{NIR}}{\rho\text{GREEN}}$	Related with leaf production and stress
Modified Simple Ratio	MSR	$\frac{\left(\frac{\rho\text{NIR}}{\rho\text{RED}}\right) - 1}{\sqrt{\left(\frac{\rho\text{NIR}}{\rho\text{RED}}\right)} + 1}$	A combination of renormalized NDVI and SR to improve sensitivity to vegetable characteristics
Simple ratio	SR	$\frac{\rho\text{NIR}}{\rho\text{RED}}$	Ratio of NIR scattering to chlorophyll and light absorption used for simple vegetation distinction
Normalized Difference Red-Edge/Red	NDRER	$\frac{\rho\text{RedEdge} - \rho\text{RED}}{\rho\text{RedEdge} + \rho\text{Red}}$	Modification of NDVI, using Red-Edge instead of NIR.

Structure Intensive Pigment Index 2	SPI2	$\frac{\rho\text{NIR} - \rho\text{GREEN}}{\rho\text{NIR} - \rho\text{RED}}$	Index used in areas with high variability in canopy structure
Leaf Chlorophyll Index	LCI	$\frac{\rho\text{NIR} - \rho\text{RedEdge}}{\rho\text{NIR} + \rho\text{RED}}$	Index to assess chlorophyll content in areas of complete leaf coverage.

Note: Agapiou et al., 2012, 2013, 2016; Bennet et al., 2012; Birth and McVey, 1968; Challis et al, 2009; Deering, 1978; Jordan 1969; Pearson & Miller, 1972; Verhoeven & Doneus, 2011. For use in this study, some closest Sequoia reflectance bands were substituted for the traditional narrowband wavelengths. Modified from: Moriarty *et al.,* 2019.

1.3 Plant Extraction (Image Segmentation)

Digital image processing and computer vision approaches are powerful tools for plant analysis because they allow plant physiological and physical features to be measured non-destructively with high temporal and quantitative resolution (Fahlgren *et al.,* 2015). After the image acquisition, the image analysis process starts with the extraction of the numerical data that describes the object in the image. First the background pixels must be separated from the object of interest through a process called object segmentation. The accuracy of this process decreases as the image quality decreases (Berry *et al.,* 2018).

Multiple plant segmentation methods have been proposed to handle the variation among different sensors including the use of adaptative thresholding and machine learning algorithms (Yogamangalam and Karthikeyan, 2013). Other systems were developed using a fixed threshold and image standardization method (Berry *et al.,* 2018).

Normalized Difference Vegetation Index (NDVI) has been widely used for distinguishing between plant and soil and plant species through satellite imagery. This occurs because the near infrared (NIR) combined with the red image provides a significantly higher reflectance than soil in natural light conditions (Soille, 2010). However, NDVI is known for presenting problems related to saturation at extreme values.

Aiming to design a robust segmentation algorithm that could be used in different soil conditions, the fixed threshold was avoided. Instead was used an automatic histogram segmentation that extracted the 92% higher reflectance values from the NDVI images when the NDVI values were superior to 0.1. Another filter based in the NIR image was tested but without reliable results (Figure 4).

After this step, the *bwarefilt* function was applied. This function allows extracting all connected components from the binary image, where the area of the objects is in the specified range producing a new binary image containing only the objects that meet the

criteria. (MatLab R2014b). In this case, the criteria was to extract the larger object of the image (with more connected components). This allowed the system to eliminate noises and unconnected pixels. The resulting binary image (mask) (Figure 4) was multiplied by the vegetation indices images, in order to extract just the values of VIs present in the plant tissue (Figure 5)

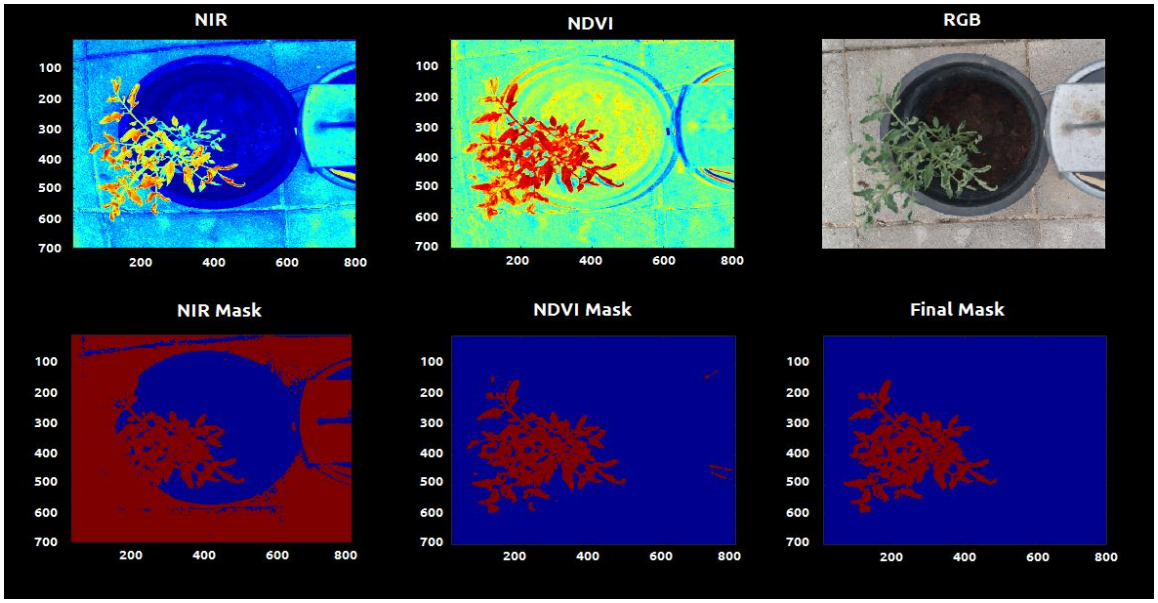

Figure 4 – Computer vision process based in NDVI image used to extract the plant from the background. Top images: Near-infrared (left), NDVI (center), and RGB (right); bottom images: binarized images.

1.4 **Morphological Analysis**

Nutrient deficiency in tomato plants can cause several symptoms besides the change in reflectance of leaves. It is common to observe changes in the plant growing behavior, specially related with morphological aspects of the leaves and shoots.

Nitrogen deficiency can cause restricted shoot growth and small erect leaflets; Phosporous deficiency can cause restricted shoot growth and small stiffed curved leaves; Deficiency of potassium can cause scorched and curled symptoms in old leaves; Zinc and Iron deficiencies can cause stunting; Boron and Calcium deficiencies can cause changes in the leaflets making them curved and deformed. Copper deficiency symptoms can be observed in the margins of leaflets and younger leaves that curl into a tube shape, the terminal leaves can become very small, stiff and contorted and the stem growth become somewhat stunted (Eysinga and Smilde, 1981).

From the binary plant datasets it is possible to measure plant size, shape, area and other features in an automated way and correlate plant phenotypes with experimental treatments (Veley et al., 2017; Liang et al., 2018).

Several other morphological properties can be extracted from binary images using the *regionprops* function in MatLab environment. This function uses the distribution of the pixels to calculate shape parameters and has been recently used for image analysis in medicine studies (Tariq *et al.* 2019), industry (Jiang *et al.,* 2019), plant pathology (Singh *et al.*, 2019) and plant growth analysis (Kim *et al.*, 2019).

These parameters can provide reliable information about the changes in the plants' area, perimeter, shape and growth behaviour.

Not all parameters resulting from the *regionprops* function were used, the description of the morphological properties used for the tomatoes plants analysis can be observed in Table 3.

Table 3 – Morphological properties calculated for the tomato plants at early stages images with different levels of organic fertilization

Morphological Property	Description
Area	Actual number of pixels in the region, returned as a scalar.
Convex Area	Number of pixels in the Image that specifies the convex hull, with all pixels within the hull filled in (set to on), returned as a binary image (logical). The image is the size of the bounding box* of the region.
Eccentricity	Eccentricity of the ellipse that has the same second-moments as the region, returned as a scalar. The eccentricity is the ratio of the distance between the foci of the ellipse and its major axis length. The value is between 0 and 1. (0 and 1 are degenerate cases. An ellipse whose eccentricity is 0 is a circle, while an ellipse whose eccentricity is 1 is a line segment.)
Diameter Equivalent	Diameter of a circle with the same area as the region, returned as a scalar. Computed as $\sqrt{4 * \frac{Area}{\pi}}$.
Euler Number	Number of objects in the region minus the number of holes in those objects, returned as a scalar.
Extent	Ratio of pixels in the region to pixels in the total bounding box*, returned as a scalar. Computed as the Area divided by the area of the bounding box*.
Filled Area	Number of on pixels in Filled Image, returned as a scalar.

Orientation	Angle between the *x*-axis and the major axis of the ellipse that has the same second-moments as the region, returned as a scalar. The value is in degrees, ranging from -90 degrees to 90 degrees.
Major Axis Length	Length (in pixels) of the major axis of the ellipse that has the same normalized second central moments as the region, returned as a scalar.
Minor Axis Length	Length (in pixels) of the minor axis of the ellipse that has the same normalized second central moments as the region, returned as a scalar
Perimeter	Distance around the boundary of the region returned as a scalar. This function computes the perimeter by calculating the distance between each adjoining pair of pixels around the border of the region
Solidity	Proportion of the pixels in the convex hull that are also in the region, returned as a scalar. Computed as Area/ConvexArea

*Bounding box: Smallest rectangle containing the region.

1.5 Statistical Analysis

The experiment used randomized blocks, with four treatments and six repetitions. Each plot was composed of six vases. The statistical analysis carried out through the ANOVA and Tukey's test at 1% of probability for average comparisons using the statistical and machine learning toolbox from MatLab software.

For the significant predictor factors, a functional boxplot and a regression analysis (using the week means) was performed in the same software.

Results and Findings

Images were collected weekly (one image per plant) during 8 weeks. The segmentation of the plant tissue from the background was needed to quantify the spectral response from each plant and to calculate the mean values of the evaluated parameters. This process also enabled the morphological analysis of the plant growth behavior.

Multiple segmentation codes were tested to remove the background, and the code based on the Normalized Difference Index was the most efficient. All the other bands (red, red edge and green) alone were not able to differentiate the plant tissue from the background.

The vegetation indices results were stored by date and treatment in image format seeking a visual confirmation of the segmentation process and a visual representation of the spectral responses (Figure 5).

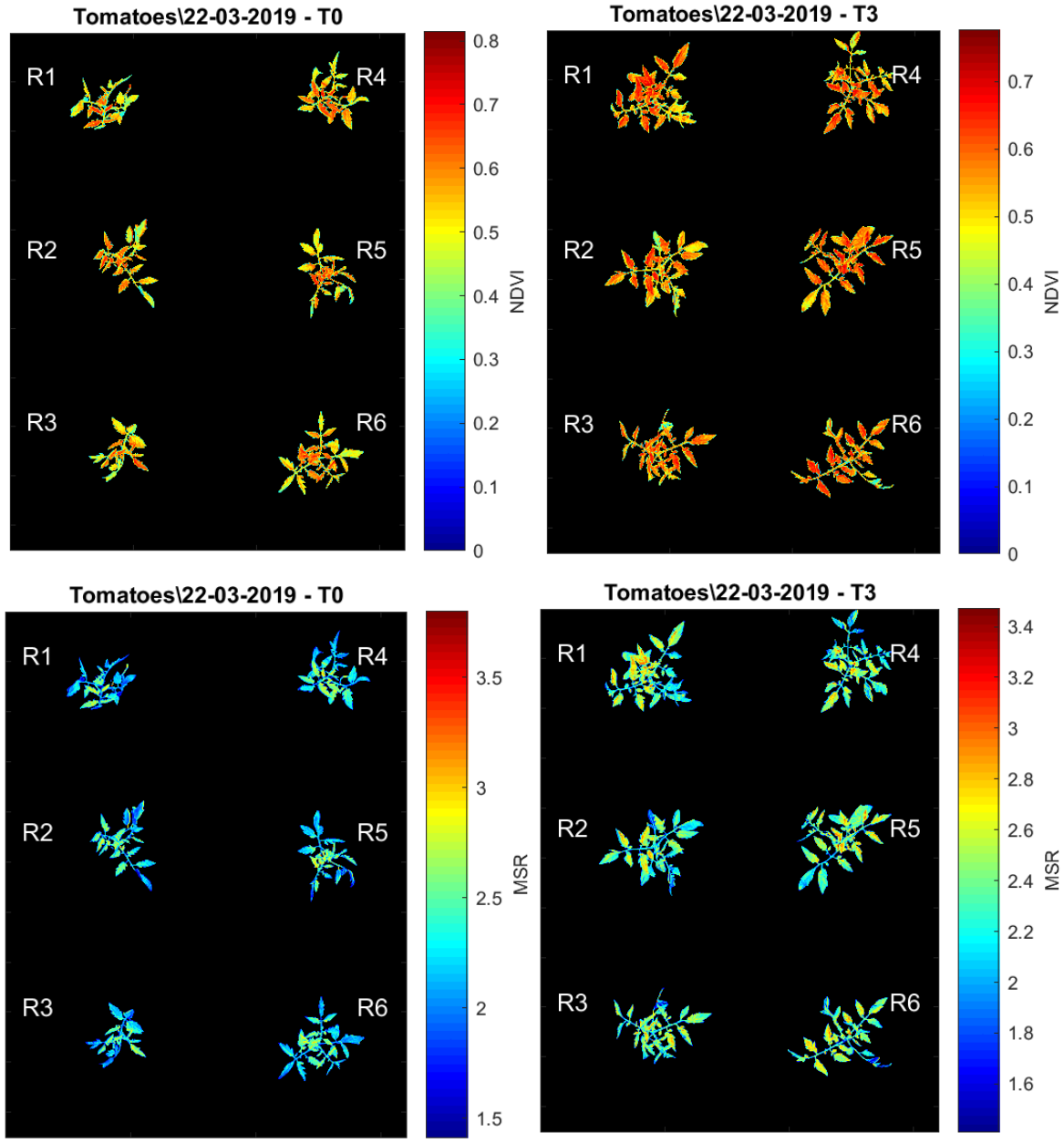

Figure 5 – Example of vegetation indices obtained through the Parrot Sequoia camera and segmentation algorithm. Top: NDVI image of the T0 treatment (left) and the T3 treatment (right). Bottom: Modified Simple Ratio image of the T0 treatment (left) and the T3 treatment (right)

The images were taken in the same position during the weeks in order to observe the growth behavior of the plants in the different treatments. Both aspects could be observed during time: morphological traits and vegetation indices (Figure 6).

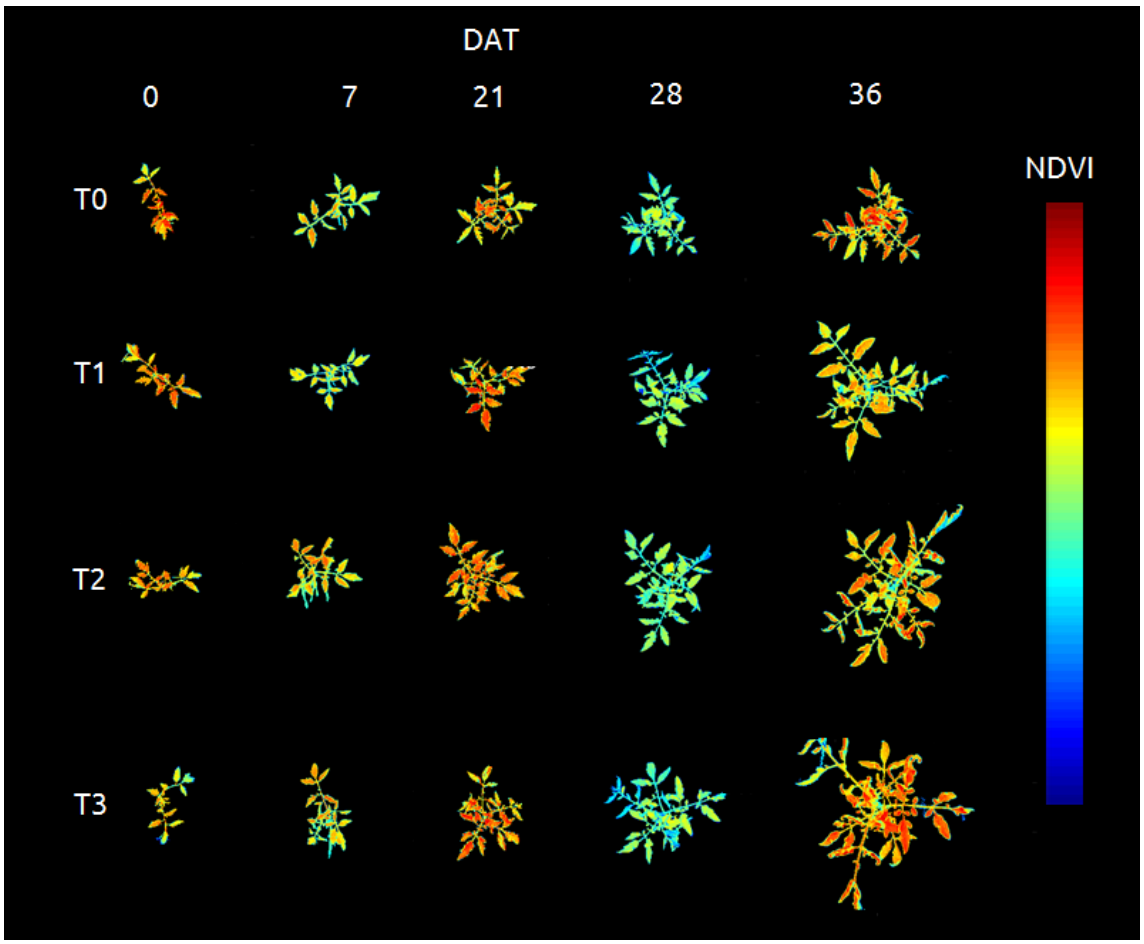

Figure 6 – Evolution of the morphology and Normalized Difference Vegetation Index of the tomato plants according to the fertilization treatments and the DAT (days after transplant).

Boxplots were created for each treatment and each date in order to observe the dispersion of the Vegetation Indices mean values and morphological parameters for the different treatments. Some examples of the measured parameters can be observed below (Figure 7).

In the boxplots, the red line indicates mean values, the superior blue line indicates the 3rd quartile of values, and the lower blue line indicates 1st quartile. The superior and inferior black lines indicate maximum and minimum values, while the red crosses indicate outliers.

The average values of the different vegetation indices per plant were calculated and compared during each week of the experiment using ANOVA and Tukey test with 99% of confidence (Table 4).

The average values of the morphological parameters were also calculated, and an ANOVA test was performed with 99 % of confidence (Table 5).

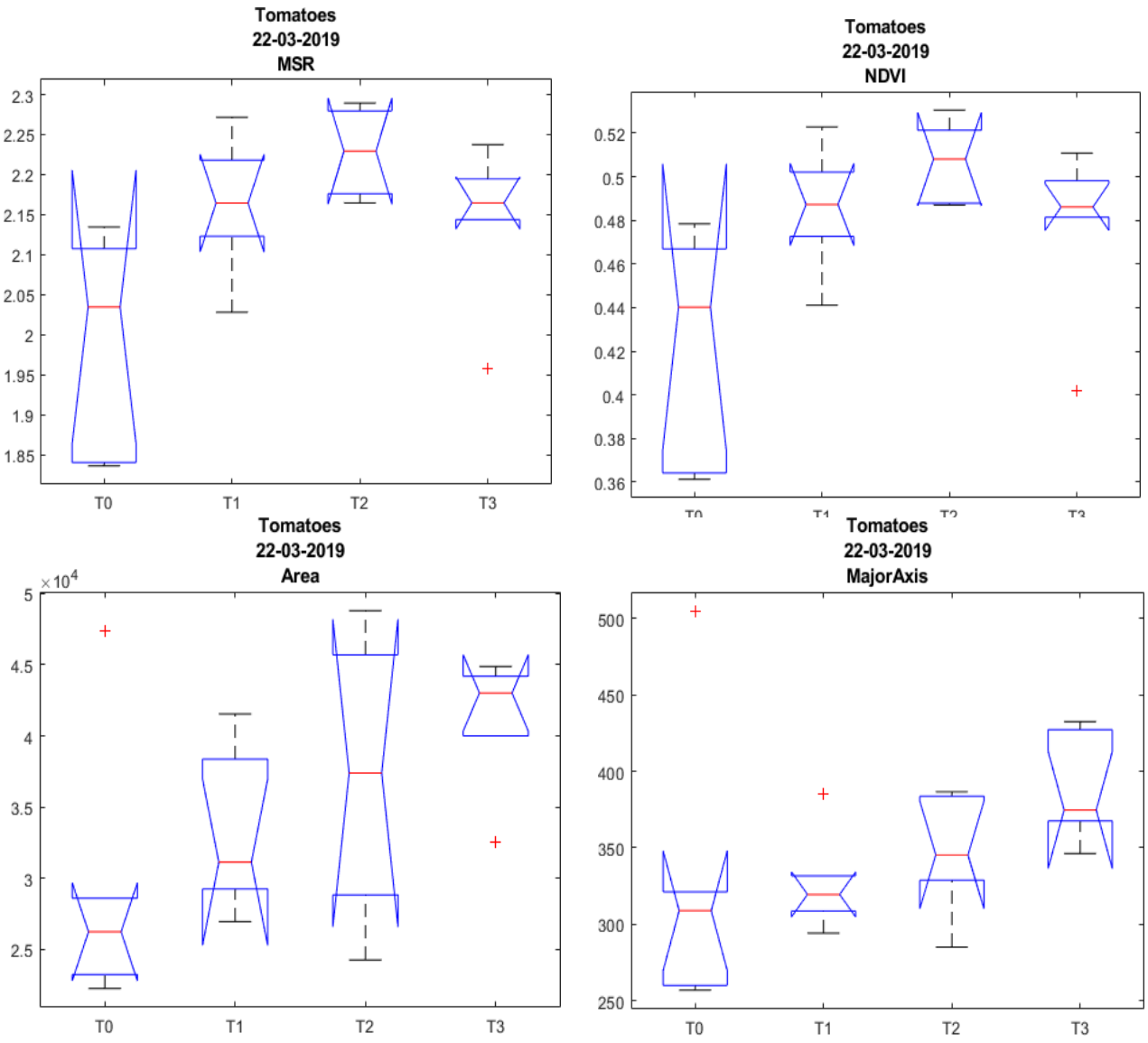

Figure 7 – Examples of boxplots created for each week. *(T0: control, T1: 25% of recommended dose, T2: 50% of recommended dose, T3: recommended dose*

Table 4 – Significance ANOVA test with 99% of probability for the relation between Vegetation Indices with the fertilization treatments per week (ns: non-significant, +: significant).

	Time after transplant (Days)							
	08-mar	15-mar	22-mar	29-mar	05-abr	12-abr	19-abr	26-abr
	0	7	14	21	28	36	43	50
NDVI	ns	ns	ns	ns	ns	ns	+	+
GNDVI	ns	ns	ns	ns	ns	ns	+	ns
RENDVI	ns	ns	ns	ns	ns	ns	ns	ns
NDRER	ns	ns	ns	ns	ns	ns	ns	ns
OSAVI	ns	ns	ns	ns	ns	ns	+	+
NLI	ns	ns	ns	ns	ns	ns	ns	ns
LCI	ns	ns	ns	ns	ns	ns	ns	ns
SR	ns	ns	ns	ns	ns	ns	+	+
MSR	ns	ns	ns	ns	ns	ns	+	+
GRVI	ns	ns	ns	ns	ns	ns	+	+
RGRI	ns	ns	ns	ns	ns	ns	ns	ns
SPI2	ns	ns	ns	ns	ns	ns	+	ns

Table 5 – Significance ANOVA test with 1% of probability for the relation between Morphological aspects derived from multispectral images with fertilization treatments per week (ns: non-significant, +: significant).

	Time after transplant (Days)							
	08-mar	15-mar	22-mar	29-mar	05-abr	12-abr	19-abr	26-abr
	0	7	14	21	28	36	43	50
Area	ns	ns	ns	+	+	+	+	+
MajorAxisLength	ns	ns	ns	+	+	+	+	+
MinorAxisLength	ns	ns	ns	+	+	+	+	+
Eccentricity	ns	ns	ns	ns	ns	ns	ns	ns
Orientation	ns	ns	ns	ns	ns	ns	ns	ns
ConvexArea	ns	ns	ns	+	+	+	+	+
FilledArea	ns	ns	ns	+	+	+	+	+
EulerNumber	ns	ns	ns	ns	ns	+	+	ns
EquivDiameter	ns	ns	ns	+	+	+	+	+
Solidity	ns	ns	ns	ns	+	+	ns	+
Extent	ns	ns	ns	ns	+	+	ns	ns
Perimeter	ns	ns	ns	+	+	+	+	+

After this initial ANOVA analysis, the significant parameters were selected, and the *p*-values can be seen in Table 6.

Table 6 – *p*-values for the most significant parameters analyzed with multispectral images in tomato plants with different organic fertilization levels. (ANOVA Significance test 99%)

	Time after transplant (Days)							
	08-mar	15-mar	22-mar	29-mar	05-abr	12-abr	19-abr	26-abr
	0	7	14	21	28	36	43	50
NDVI	-	-	-	-	-	-	2,00E-02	5,00E-02
MSR	-	-	-	-	-	-	7,40E-02	3,00E-02
GRVI	-	-	-	-	-	-	1,30E-02	1,03E-01
Area	-	-	-	2,00E-04	3,06E-06	1,92E-07	1,82E-08	1,96E-05
MajorAxisLength	-	-	-	2,56E-06	1,04E-09	1,16E-03	8,00E-04	2,97E-06
MinorAxisLength	-	-	-	7,00E-04	1,26E-05	6,77E-06	1,58E-05	9,24E-05
ConvexArea	-	-	-	2,90E-05	2,86E-08	7,99E-07	1,88E-06	2,05E-06
FilledArea	-	-	-	2,00E-04	1,09E-05	5,53E-07	1,80E-08	3,78E-06
Perimeter	-	-	-	1,60E-03	2,17E-08	4,13E-06	3,72E-06	2,00E-04
EquivDiameter	-	-	-	6,92E-05	8,12E-07	3,34E-08	2,93E-08	8,53E-06

In order to compare the different results for each treatment, a Tukey's HSD test was performed, for the most significant parameters for each week of the experiment. The results can be seen in Table 7 and the order of the letters indicates the treatments T0, T1, T2 and T3 respectively.

Table 7 – Tukey's HSD test with 99% confidence for the relation between vegetation indices and morphological aspects derived from multispectral images with organic fertilization treatments per week.

	Time after transplant (Days)							
	08-mar	15-mar	22-mar	29-mar	05-abr	12-abr	19-abr	26-abr
	0	7	14	21	28	36	43	50
NDVI	-	-	-	-	-	-	a, ab, b, ab	a,b,ab,ab
MSR	-	-	-	-	-	-	a, ab,b,ab	a,b,ab,ab
GRVI	-	-	-	-	-	-	a, ab,b,ab	a,b,ab,ab
Area	-	-	-	a, ab, b, b	a, b, b, b	a, b, b, b	a, b, b, b	a, b, b, b
MajorAxisLength	-	-	-	a, b, b, b	a, b, b, b	a, b, b, b	a, ab,b,ab	a, b, b, b
MinorAxisLength	-	-	-	a, ab, b, b	a, b, b, b	a, b, b, b	a, b, b, b	a, b, b, b
ConvexArea	-	-	-	a, ab, b, b	a, b, b, b	a, b, b, b	a, b, b, b	a, b, b, b
FilledArea	-	-	-	a, ab, b, b	a, b, b, b	a, b, b, b	a, b, b, b	a, b, b, b
Perimeter	-	-	-	a, ab, ab, b	a, b, b, b	a, b, b, b	a, b, b, b	a, b, b, b
EquivDiameter	-	-	-	a, ab, b, b	a, b, b, b	a, b, b, b	a, b, b, b	a, b, b, b

Aiming to identify the most reliable parameters to predict the fertilization level of organic tomato, boxplots were created with the whole amount of data, without week distinction.

After that, a comparison test (Tukey's HSD), with 99% of confidence was performed.

This analysis can indicate which parameters are more robust to use in an automatic and nondestructive fertilization level analysis model.

The graphical representation of the Boxplots and Tukey's comparison test can be seen below. In the case of the morphological aspects, some of the parameters presented significant results with distinction between the control (T0) and the treatments (T1, T2 and T3) (Figure 8).

On the other hand, none of the Vegetation Indices presented a significative difference (with a 99% level of confidence) to predict the nutritional level of organic tomato plants independent of the week after transplant (Figure 9).

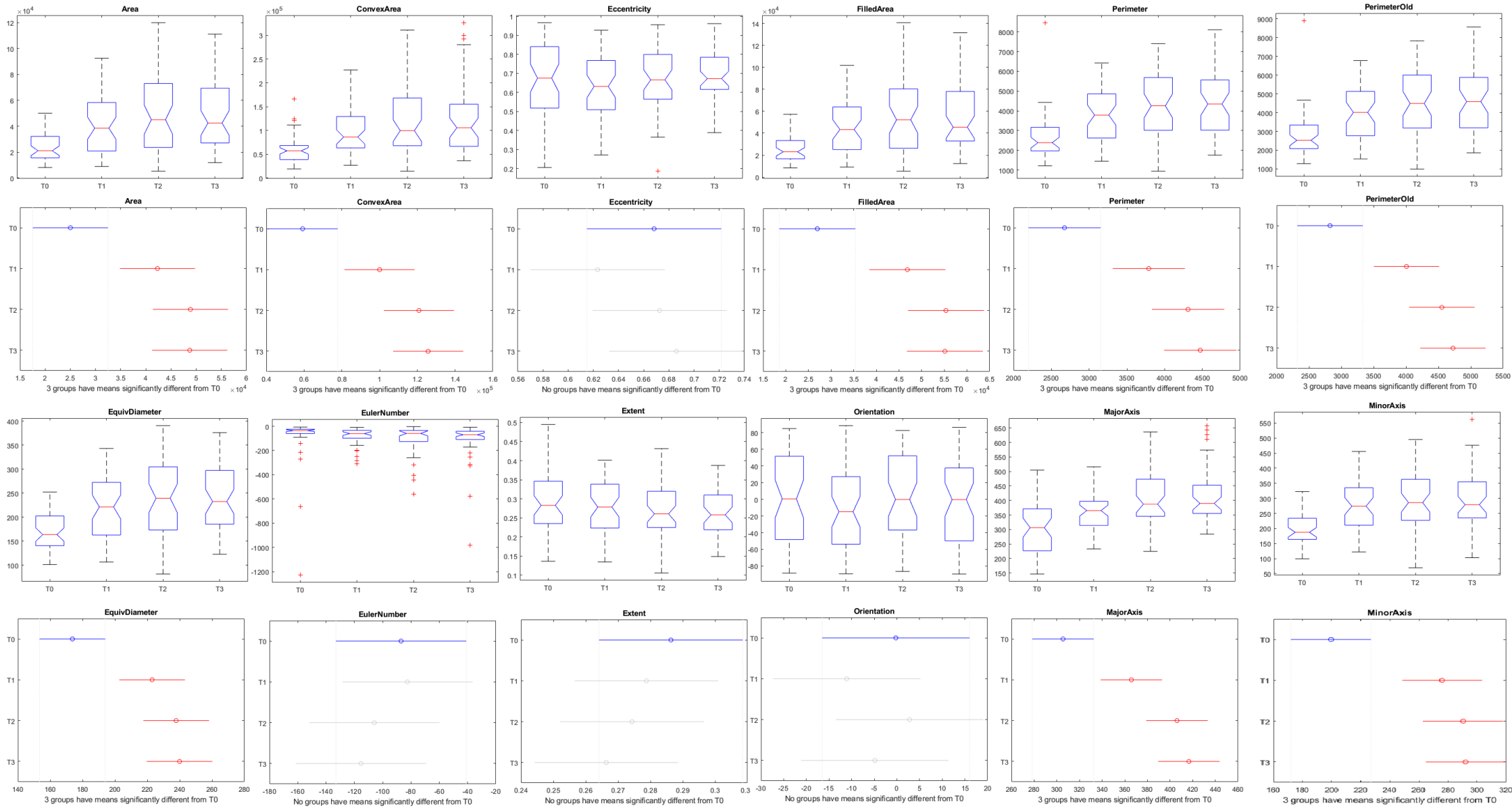

Figure 8 – Boxplots and Tukey Test with 99% of probability using all data (50 days) representing morphological parameters of tomato plants with different levels of organic fertilization

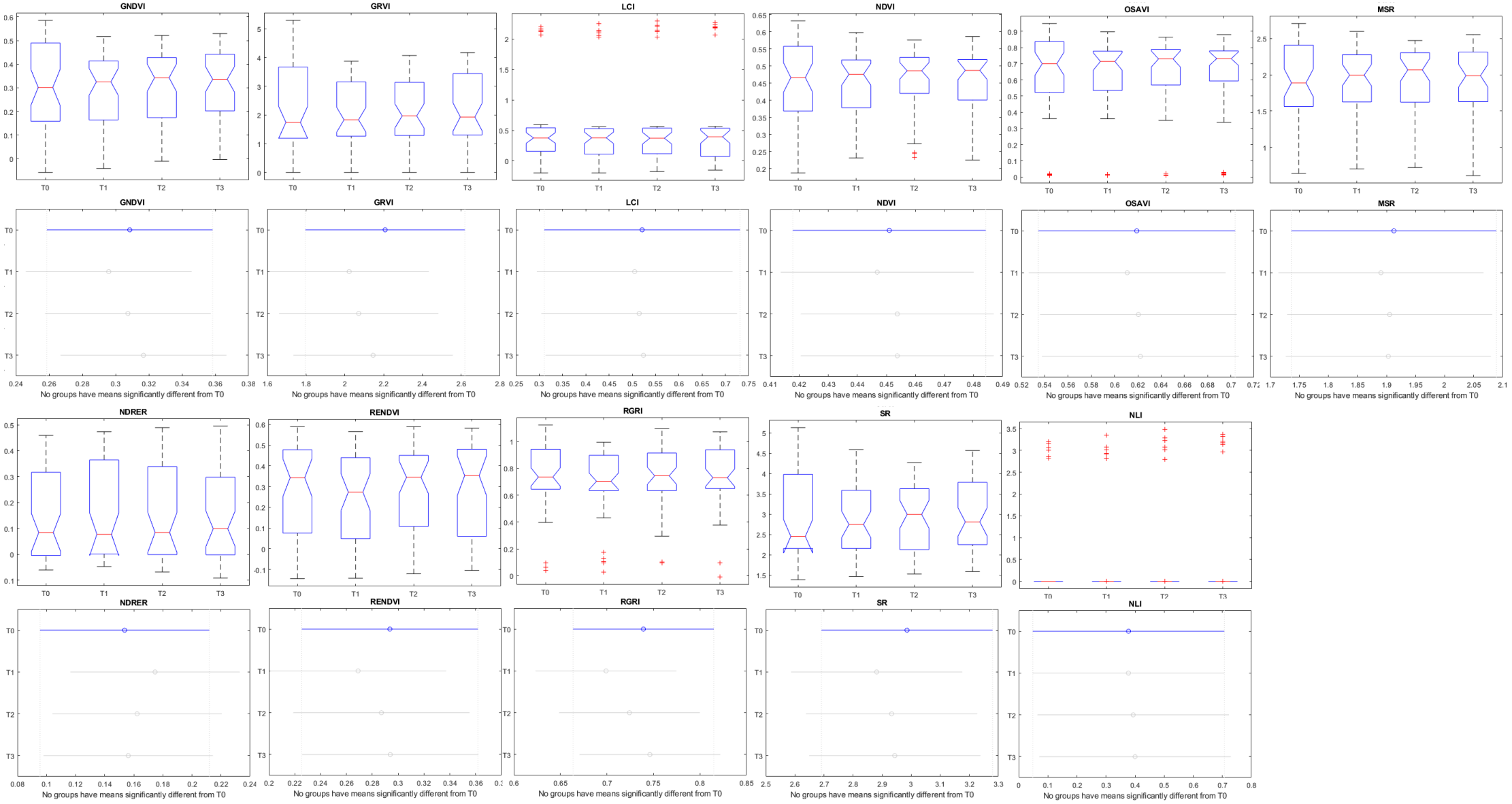

Figure 9 – Boxplots and Tukey Test with 99% of probability using all data (50 days) representing Vegetation Indices of tomato plants with different levels of organic fertilization

The results presented in Table 5, Figure 8 and Figure 9 indicate that the morphological parameters are more related to the fertilization level of tomato plants at early stages than the spectral responses. These parameters were selected to create regression models in order to predict the nutritional status of the tomato crop.

The regression models were created using the MatLab function *curvefit*, the mean values of the control (T0) and the recommended dose (T3), for the first five weeks and excluding outliers. The selected parameters were: Area, Filled Area, Convex Area, Perimeter, Equivalent Diameter, Major Axis Length and Minor Axis Length (Table 8 and Figure 10).

Table 8 – Linear and polynomial regressions correlating morphological parameters acquired using multispectral images with weeks after transplant in different organic fertilization levels in tomato plants at early stages.

Parameter	*Tr.*	*Regression*	R^2
Area	T0	$f(x) = 10070x + 26550$	0,937
	T3	$f(x) = 2825x^2 + 3078x + 8909$	0,983
Filled Area	T0	$f(x) = 6766x + 8284$	0,953
	T3	$f(x) = 3118x^2 + 2072x + 13130$	0,977
Perimeter	T0	$f(x) = 164.5x + 2211$	0,559
	T3	$f(x) = 381.7x^2 - 1065x + 3265$	0,941
Eq. Diameter	T0	$f(x) = 21.93x + 114.4$	0,938
	T3	$f(x) = 52.65x + 80.43$	0,971
Convex Area	T0	$f(x) = 2984x^2 - 8845x + 56880$	0,957
	T3	$f(x) = 19530x^2 - 60980x + 95950$	0,992
Major Axes	T0	$f(x) = 16.53x^2 - 112.2x + 522.2$	0,933
	T3	$f(x) = 27.41x^2 - 106.9x + 452.5$	0,988
Minor Axes	T0	$f(x) = -4.833x^2 + 61.4x + 77.95$	0,976
	T3	$f(x) = 71.54x + 69.48$	0,964

Seeking for a more robust, simple and reliable prediction model, functional boxplots were created using the mean values of each plant T0 and T3 for the first four weeks and plotted together.

Functional boxplots were also created for some of the vegetation indices that showed statistical differences at least in two weeks, for example, Modified Simple Ratio (MSR) and Green Normalized Difference Index (GRVI).

The functional boxplots represent the mean data of each week without the outliers with an interval of confidence of 95% (Figure 11 and 12).

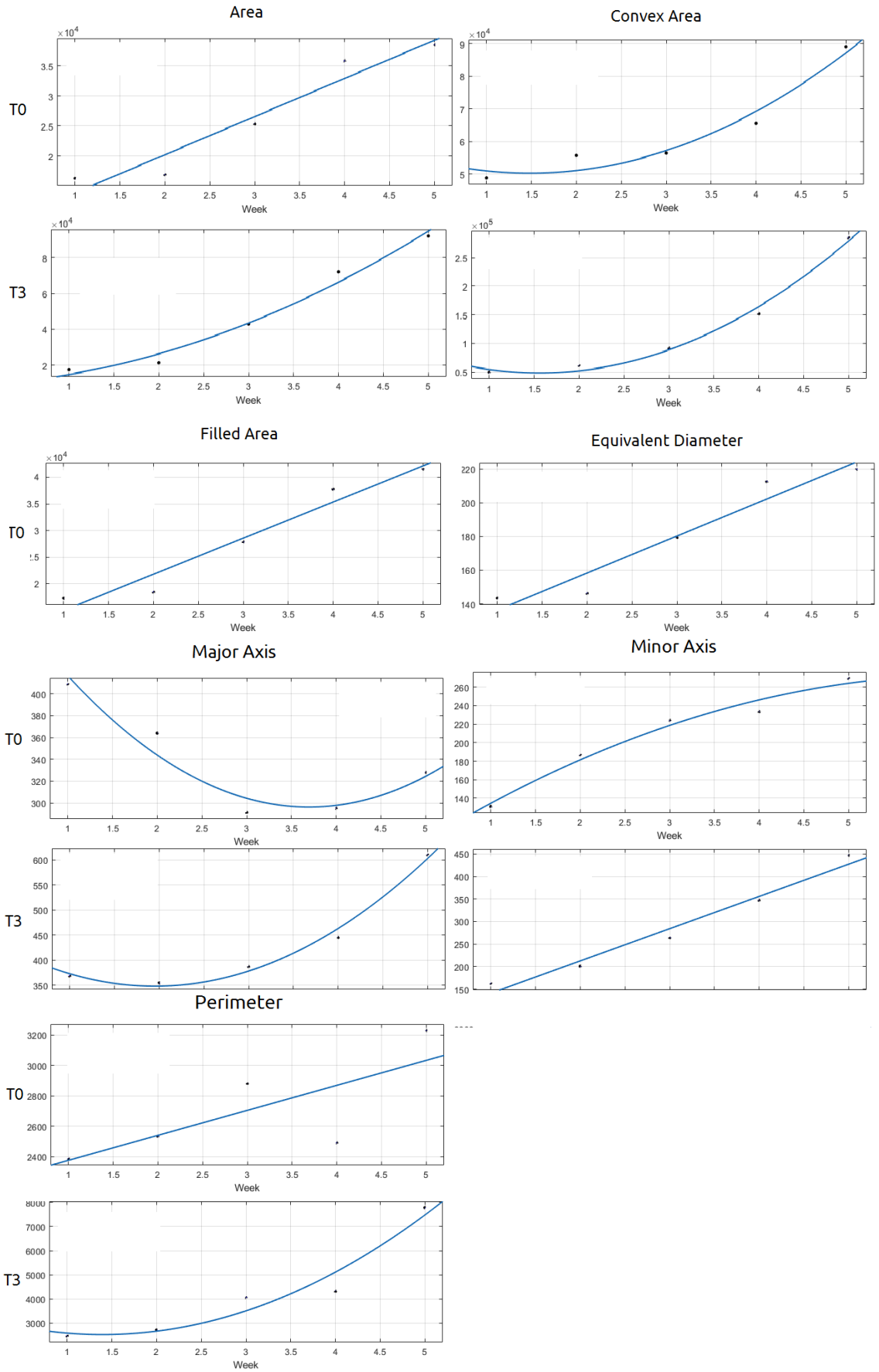

Figure 10 – Linear and Polynomial regression curves relating the morphological parameters of tomato plants acquired using multispectral images with the number of weeks after transplant and different organic fertilization levels.

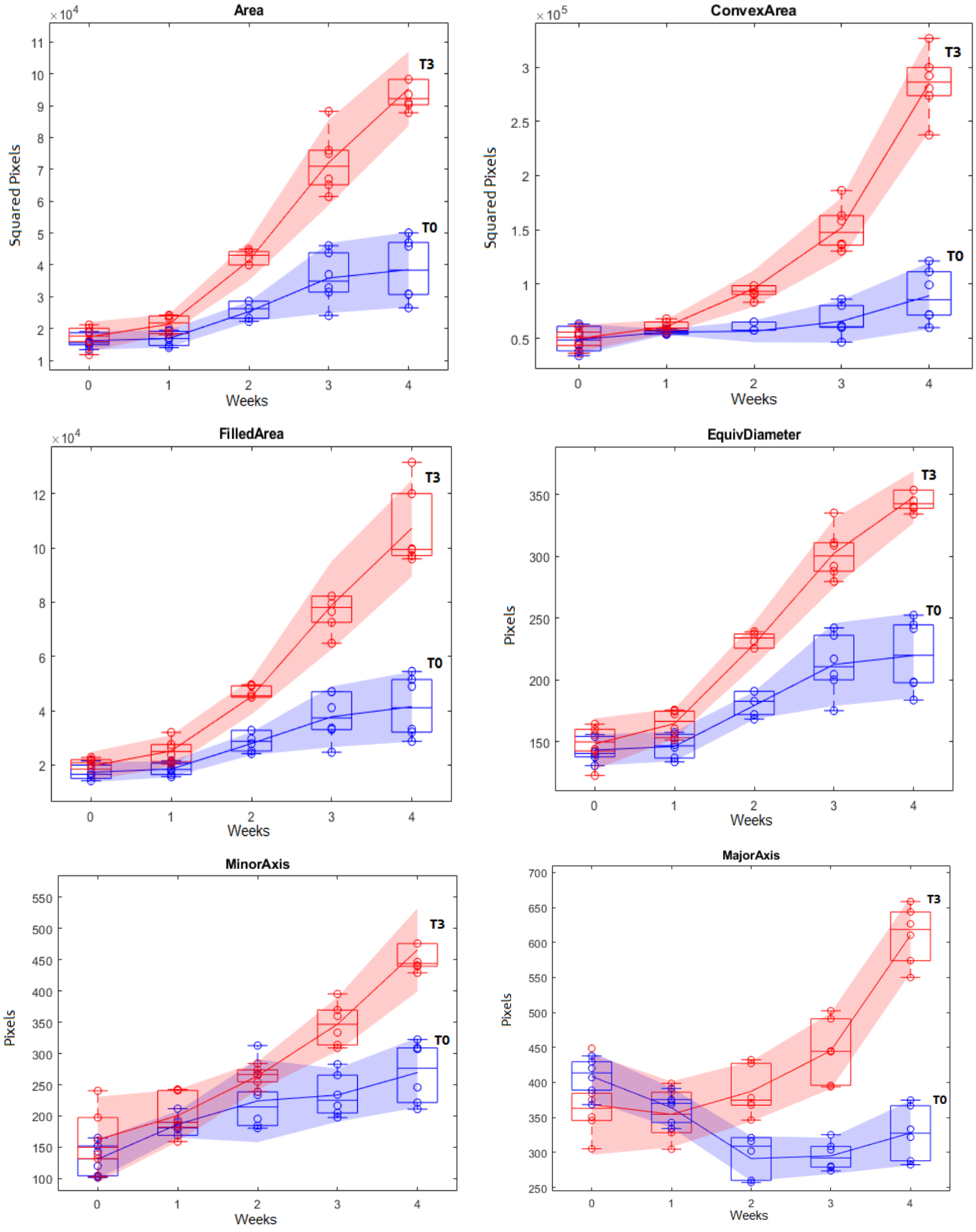

Figure 11 – Functional boxplots showing morphological responses extracted from multispectral images correlating with number of weeks after transplant and fertilization treatments with a confidence interval of 95%.

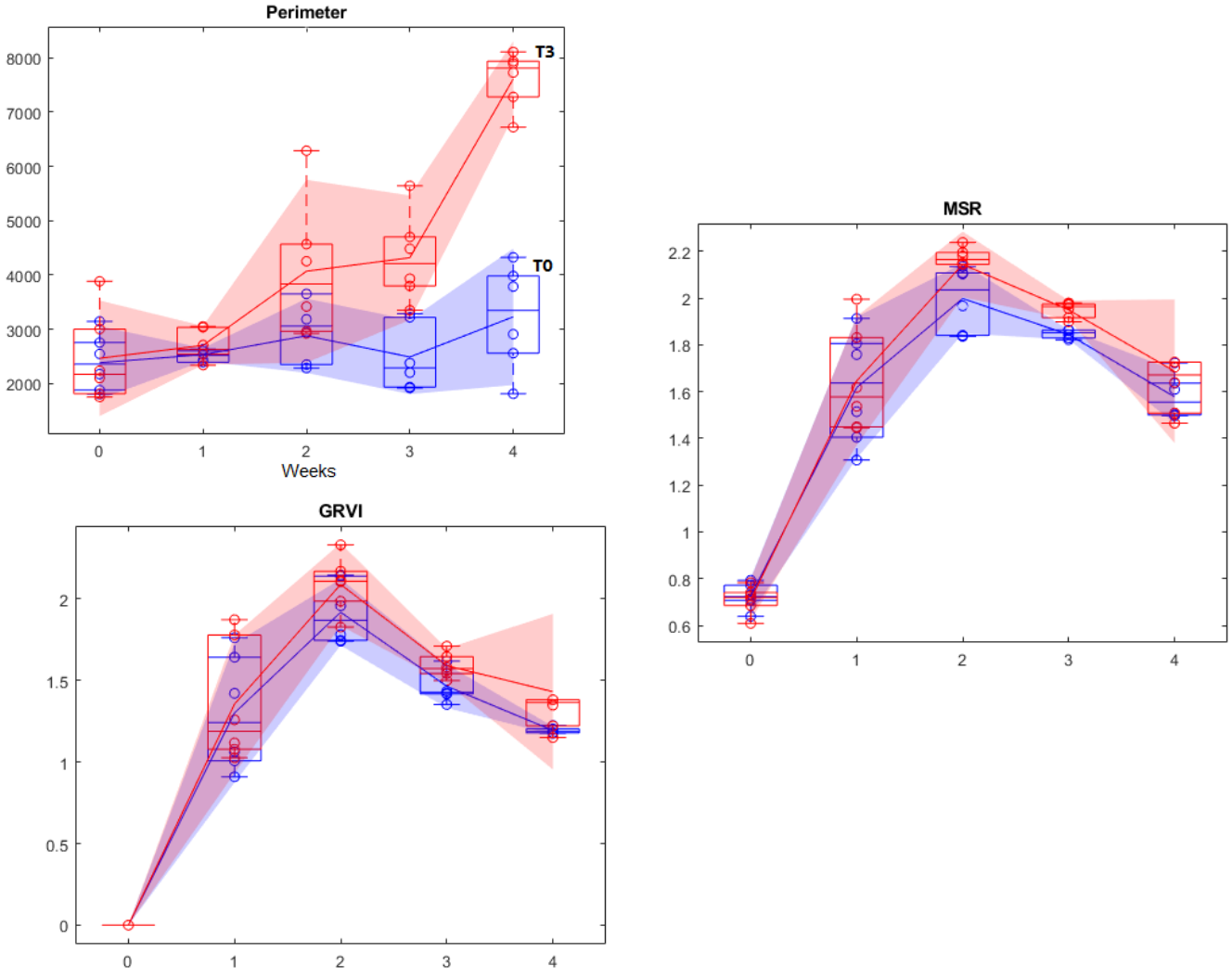

Figure 12 – Functional boxplots showing morphological and spectral responses extracted from multispectral images correlating with the number of weeks after transplant and fertilization treatments with a confidence interval of 95%.

Discussion

The system used for image acquisition showed to be effective for tomato plants at early stages. The same system can be adjusted for tomato plants at late stages and can also be used for other plant species and seedlings in different stages (depending on the height adjustments). The pre-processing technique showed to be adequate for overlay the Parrot Sequoia images in the different heights tested 0.70 cm and 1.40 cm.

The plant segmentation is the cornerstone of the image analysis at plant level. Diverse authors used multispectral images to access the nutritional level of the plants. These works usually are focused in small zones or areas, or in multiple plants in a parcel as the

minimum management unit. In order to perform precise fertilization at plant level, the segmentation and extraction of the plant of interest must be also precise.

The algorithm developed using the Normalized Difference Index was able to distinguish plant tissue from soil, vase, floor and metal platform extracting the whole plant apart of the background (Figures 3, 4 and 5). The use of NDVI for vegetation extraction and monitoring is widely used for satellite imagery (Bhandari *et al*., 2012; Manakos & Braun 2014), and this study proves that can also be used with high-resolution plant images.

The code was tested in three different conditions with different levels of efficacy in extract the plant. In 100% of the images the code was able to extract the whole plant. Using black pots without the black background the code was able to extract the whole plant without any noise with efficacy of 87,5%. Using a brown pot with black background, the code was able to extract only plant tissue with an efficacy of 96.8%. However, using brown pots without black background the code reduced the efficacy in extract only plant tissue to 54,17%.

The visual inspection was needed to guarantee that the plants were well-segmented and also provides the distribution of the Vegetation Indices intensity through the leaf tissue. The segmentation also allows morphological analysis during the time, and this system can be useful for digital phenotyping projects.

The Vegetation Indices used in this study did not show significant differences between the treatments during the initial stages of the plant development, only in the 6^{th} and 7^{th} weeks after the transplant differences between T0 and T2 and T0 and T1 respectively without practical applications. Among the vegetation indices studied the NDVI, GRVI, OSAVI, SR and MSR showed the differences.

Different results were found by Padilla *et al*. (2015), that using the Crop Circle ACS 470 and the SPAD 502 sensors concluded that the vegetation indices based on the red band (NDVI and Red Vegetation Index) were the best predictors for nitrogen levels in tomatoes maintaining the relationships during the crop. According to the authors, the SPAD readings, the GNDVI and the GVI were good predictors of the nitrogen status of the crop in the beginning of the cycle, with low accuracy in the later part of the crop cycle.

Using the same sensor (Circle ACS 470) and guided sampling method, Fortes *et al.* (2015), developed a yield prediction map of tomato crop. Their study used the NDVI index as a predictor parameter and the correlation between the vegetation index and the yield were of 0.67 and 0.71 in two different regions of Spain.

Other study conducted by Oliveira *et al*. (2019) showed the possibility to use vegetation indices to improve the use of nitrogen fertilization in tomatoes cultivated in protected environment. Applying the spectral sensors ASD Field Spec HandHeld 2, and the Minolta SPAD 502, the authors compared the spectral response of tomato plants in the reference plot and with lower levels of nitrogen fertilization. The use of NDVI and the SPAD measurements as a nitrogen level parameter allowed to reduce significantly the use of nitrogen fertilization maintaining the same yield levels and fruit quality compared to the reference plot.

On the other hand, during three years of field trials with different levels of nitrogen fertilization Gianquinto *et al*. (2011) evaluated vegetation indices of tomato plots through the use of a multispectral radiometer (MSR-87, Cropscan Inc.). In their study, sixteen vegetation indices were analyzed and the NDVI did not show a strong correlation with nitrogen concentration on leaves. It was concluded that the best vegetation index for nitrogen evaluation in tomato was the relation between NIR and the reflectance present in the range of 560nm (NIR/R_{560}).

Some reasons can be responsible for the divergence observed between results. The type of fertilizer is one of them, in all the previous studies, mineral nitrogen fertilization was used. This type of fertilizer is more soluble and less stable and can be absorbed and translocated faster than the organic amendments. The crop stage during the measurements can also be a factor. In the previous studies, the measurements started after the 29^{th} day after transplant where the plants were developed more, and the deficiencies symptoms were more present. The type of sensor is also an important factor because this was the first study to use the Parrot Sequoia sensor at plant level to monitor nutrient deficiency in tomatoes. Kipp *et al.* (2013), showed the differences in measurements in different commercial spectral sensors for nitrogen management, and among the studied factors was concluded that the measuring distance, the device temperature and the light intensity can influence the performance of the sensors.

In order to optimize the use of the spectral information acquired by the Parrot Sequoia camera for monitoring the nutrient content of tomato plants at early stages, a principal component analysis approach can be used. This methodology uses orthogonal transformations to convert the spectral measurements at different wavelengths into an orthogonal system of eigenvectors. This approach combined with multiple linear regression allows to create a new vegetation indices, reconstruct the leaf reflectance spectra and predict the leaf biochemical contents with high accuracy (Liu *et al.*, 2017).

The most interesting results were obtained through the analysis of the morphological traits of the tomato plants. Seven of the twelve aspects analyzed showed significant difference between the control and the fertilized treatments.

Only 3 weeks after the transplant, the plants started to exhibit a significant difference in the plant area, convex area, filled area, minor axis length and equivalent diameter discriminating T3 and T2 of T1 and the control. In the same period, the perimeter was significantly different between the recommended dose T3 and the control, without difference between T2 and T1.

The length of the major axis could discriminate between the control against the treatments but not between the treatments already in the 3rd week.

In the following weeks, from the 4th week to the end of the study, all the seven morphological traits (Area, Convex Area, Filled Area, Equivalent Diameter, Perimeter, Minor Axis Length and Minor Axis Length) showed significant differences between the control and the treatments, except for the major axis length in the 7th week after transplant.

These results are in agreement with the results described in the literature. Mooy *et al. (*2019), showed the positive influence of soluble organic fertilizer in tomato plant height and the number of leaves. Other studies also demonstrated that the nitrogen and phosphorous fertilization influences the fresh shoot weight, plant height, stem diameter, leaf number and leaf area of tomato seedlings (Nicola and Basoccu, 1992; Basoccu and Nicola, 1994;, Melton and Dufault, 1991).

In field trials, the nitrogen fertilization produced an increase in the leaf area index and in the above-ground weight of tomato plants (Scholberg *et al.,* 2000; Elia and Conversa, 2012) and the use of NPK induce an increase in plant height and in the number of leaves (Hariyadi *et al.,* 2019).

Besides of the slight difference in the morphological parameters between the fertilized treatments T1, T2 and T3 there was no significant difference with 1% of probability, because of that for the functional boxplot analysis the treatment with the recommended dose (T3) was chosen for comparison with the control (T0).

The use of functional boxplots as a predicted model it is interesting because they can exclude outliers and be used as a threshold parameter (Cai *et al.,* 2000) for recommendation at field level. As can be observed the functional boxplots displays the range of the observed values until the 4th week after transplant and not until the 7th week.

At the 5th week the plants were too high to be observed with 0.70 m height as was planned for the robotic prototype, so the camera bracket was set for a 1.4 m height. This adjustment in the camera distance cause differences in the relationship between morphological parameters and the number of pixels.

The higher distance between the camera and the plant makes the plant image smaller, so the leaf area represented by the pixel area became smaller than with the distance of 0.70 m. In order to model the data, regression analysis using the mean values was performed, so the results could be extrapolated for the next weeks.

Conclusions

-The computer vision methodology developed in this master thesis was suitable for monitoring the development of tomato var. Mina F1 at early stages with different levels of organic fertilization in a protected environment. The methodology involves consecutive steps and using an automatic and non-destructive approach provides several morphological and spectral aspects of the plants that can be used in a robotic platform.

-After the pre-processing, the NDVI threshold showed to be crucial and effective for plant extraction. Among the several spectral (vegetation indices) responses observed, the NDVI, OSAVI, Simple Ratio, GRVI and Modified Simple Ratio were the only ones that showed a small difference between treatments in the 6th and 7th week after transplant, but without practical applications.

-Studying the evolution of crop by using multiples images allowed to extract several morphological features. The automatic morphological analysis was able to distinguish between the control and the fertilized treatments from the 3rd week after transplant until the end of the experiment with 99% of confidence according to the Tukey's Honest Significant Differences test.

-Among the studied morphological parameters, area, convex area, filled area, perimeter, major axis length, minor axis length and equivalent diameter showed to be useful to distinguish between the control and fertilized treatments. Convex area was the parameter that presented the highest difference between control and the fertilized plants according to the functional boxplot analysis.

-This was the first study to relate the use of morphological features extracted automatically with the organic fertilization level of tomato plants. The image analysis system was able to distinguish plant tissue apart soil, floor and metal structures, therefore most of the image processing steps can be extrapolated to other vegetable cultures, although future analysis is necessary to evaluate its robustness. Moreover, the

Parrot Sequoia Camera fulfilled the requirements to be used in the robotic platform and besides be originally developed for aerial images this study proved the capacity of its use at short distances.

-Additionally, the same methodology can be used for analyzing other aspects related with morphology features in tomato plants, such as disease severity, hydric and salinity stress or any environmental modification that can cause aboveground changes in the morphology or spectral responses of vegetable plants. This technique has potential to be used in many branches of plant health studies and provides an innovative and automatic way to measure the severity of an “abiotic disease”.

-In a subsequent investigation, we are developing an extended version of the methodology to be applied using the robotic platform at field level. Trials are being conducted in an experimental line with different vegetable crops to study the best image acquisition interval in a scenario with movement. Other trials using the robotic platform are being conducted in an experimental field area with different crops such as onion, pumpkins, tomatoes and zucchini with different levels of fertilization. In these trials the multispectral camera is being integrated with laser sensors (Lidar) for a multiscale analysis of the crops.

Bibliography

AMPATZIDIS, Y.; DE BELLIS, L.; LUVISI, A. (2017). iPathology: robotic applications and management of plants and plant diseases. *Sustainability*, 9(6): 1010-1024.

ÁVILA-NAVARRO, J.; FRANCO, C. A.; RASMUSSEN, J., & NIELSEN, J. (2019). Color Classification Methods for Perennial Weed Detection in Cereal Crops. *Progress in Pattern Recognition, Image Analysis, Computer Vision, and Applications*, 117-123.

AGRIOS, G. N (2005). Introduction to plant pathology. Elsevier Academic Press Publication. 257-262 pp.

BASOCCU, L.; NICOLA, S. (1994) Supplementary light and pretransplant nitrogen effects on tomato seedling growth and yield. *Hydroponics and Transplant Production* 396:313-320.

BHANDARI, A.K.; KUMAR, A.; SINGH, K.; (2012) Feature Extraction using Normalized Difference Vegetation Index (NDVI): a Case Study of Jabalpur City. *Procedia Technology 6*: 612-621.

BERRY, J. C., FAHLGREN, N., POKORNY, A. A., BART, R. S., & VEEY, K. M. (2018). An automated, high-throughput method for standardizing image color profiles to improve image-based plant phenotyping. *PeerJ*, 6: e5727.

BROWN, John Frederick; OGLE, H. J. (1997) Plant pathogens and plant diseases. Published by Rockvale Publications for the Division of Botany, University of New England. 156-157pp.

CANDIAGO, S.; REMONDINO, F.; De GIGLIO, M.; DUBBINI, M. & GATTELI, M. (2015). Evaluating multispectral images and vegetation indices for precision farming applications from UAV images. *Remote sensing*, 7(4):4026-4047.

CAVENDER-BARES, K.; BARES, C. (2019) **Robotic platform and method for performing multiple functions in agricultural systems**. U.S. Patent Application n. 16/188,422, 14 mar. 2019.

CHAWADE, A.; van HAM J.; BLOMQUIST, H., BAGGE, O., ALEXANDERSON, E., & ORTIZ, R. (2019). High-Throughput Field-Phenotyping Tools for Plant Breeding and Precision Agriculture. *Agronomy,* 9(5): 258-276.

CHEN, C.; PAN, J., & LAM, S. K. (2014). A review of precision fertilization research. *Environmental earth sciences*, 71(9):4073-4080.

CHRISTENSEN, S.; SØGAARD, H. T.; KUDSK, P.; NØRRENMARK, M., LUND, I.; NADIMI, E. S., & JØRGENSEN, R. (2009). Site-specific weed control technologies. *Weed Research*, 49(3):233-241.

DU, Y.D.; NIU, W.Q.; GU, XB.; ZHANG, Q.; CUI, B.J.(2018). Water-and nitrogen-saving potentials in tomato production: A meta-analysis. *Agricultural water management*, 210:296-303.

FAHLGREN N., GEHAN, M. A., & BAXTER, I. (2015). Lights, camera, action: high-throughput plant phenotyping is ready for a close-up. *Current opinion in plant biology*, 24:93-99.

FORTES, R.; PRIETO, M.H.; GARCÍA-MARTIN, A.; CÓRDOBA,A.; MARTÍNEZ, L.; CAMPILLO,C. (2015). Using NDVI and guided sampling to develop yield prediction maps of processing tomato crop. Spanish Journal of Agricultural Research. 16(1):1-9.

FREIDENREICH, A.; BARRAZA, G.; JAYACHANDRAN, K., & KHODDAMZADEG, A. A. (2019). Precision Agriculture Application for Sustainable Nitrogen Management of *Justicia brandegeana* Using Optical Sensor Technology. *Agriculture,* 9(5): 98

GERHARDS, R.; OEBEL, H. (2006) Practical experiences with a system for site-specific weed control in arable crops using real-time image analysis and GPS-controlled patch spraying. *Weed research*, 46(3):185-193.

GHORBANI, R.; KOOCHEKI, A.; BRANDT, K.; WILCOCKSON, S.; & LEIFERT C. (2010). Organic agriculture and food production: Ecological, environmental, food safety and nutritional quality issues, in S*ociology, Organic Farming, Climate Change and Soil Science* Ed. Springer 77pp.

GIANQUINTO, G.; ORSINI, F.;FECONDINI, M.; MEZZETTI, M.,; SAMBO, P.; BONA, S.; (2011). A methodological approach for defining spectral indices for assessing tomato nitrogen status and yield. *European Journal of Agronomy* 35(3):135-143.

GRIMSTAD, Lars; FROM, Pål. (2017). The Thorvald II agricultural robotic system. *Robotics*, 6(4): 24 -38.

HARIYADI, B. W.; NISAK, F.; NURMALASARI, I. R.; KOGOYA, Y. (2019). Effect of Dose And Time of Npk Fertilizer Application on The Growth And Yield of Tomato Plants (*Lycopersicum Esculentum* Mill). *Agricultural science,* 2(2): 101-111.

HIDALGO-BAZ, M.; MARTOS-PARTAL, M.; GONZÁLEZ-BENITO, Ó. (2017). Attitudes vs. purchase behaviors as experienced dissonance: The roles of knowledge and consumer orientations in organic market. *Frontiers in psychology*, 8: 248-236.

IFOAM, LANG, L. (2019) Farming without agro-chemicals. The stance of organic farmers. STOA Workshop 1-14 pp.

INDEXBOX (2017). U.S. Organic Tomato Market, Analysis and Forecast to 2025. IndexBox Marketing and Consulting 1-51.

JIANG, J. (2019) Design of Meshing Assembly Algorithms for Industrial Gears Based on Image Recognition. In: *International Conference on Advanced Information Systems Engineering.* Springer, Cham 64-72 pp.

KENNELLY, M., O'MARA, J., RIVARD, C., MILLER, G.L. and D. SMITH. (2012). Introduction to abiotic disorders in plants. American Phytopatological Society, *The Plant Health Instructor*.

KIM, S. L., CHUNG, Y. S., JI, H., EE, H., CHOI, I., KIM, N., ... & LEE, G. S. (2019). New Parameters for Seedling Vigor Developed via Phenomics. *Applied Sciences*, *9*(9):1752.

KING, A. (2017). The future of agriculture. *Nature*, *544*(7651): S21-S23.

KIPP, S., MISTELE, B.; SCHIMIDHALTER, U. (2014). The performance of active spectral reflectance sensor as influenced by measuring distance, device temperature and light intensity. *Computers and Electronics in Agriculture,* 100:24-33.

KITIC, G.; TAGARAKIS, A.; CSELYUSZKA, N., PANIC, M.; BIRGERMAJER S.; SAKULSKI, D., & MATOVIK, J. (2019). A new low-cost portable multispectral optical device for precise plant status assessment. *Computers and Electronics in Agriculture*, 162: 300-308.

KRISTENSEN, H. L. (2019). Strip-cropping and recycling of waste for biodiverse and resource-efficient intensive vegetable production. Poster at: Core Organic Cofund Research and Outreach Seminar, CIHEAM Bari, 29. January 2019.

LIANG Z.; PANDEY P.; STOERGER V.; XU Y.; QIU Y.; Ge Y.; SCHNABLE C. (2018). Conventional and hyperspectral time-series imaging of maize lines widely used in field trials*. Gigascience* 7(2):1-11

LIU L.; SONG, B.; ZHANG, S.; LIU, X.; (2017) A Novel Principal Component Analysis Method for the Reconstruction of Leaf Reflectance Spectra and Retrieval of Leaf Biochemical Contents. *Remote sensing 9(1113):1-23.*

MANAKOS I.; BRAUN, M. (2014). Land use and Land Cover Mapping in Europe: Practices & Trends, Remote Sensing and Digital Image Processing 18. Springer Science and Business Media. 363-381pp.

MELTON, R. R.; DUFAULT, R.J. (1991). Nitrogen, phosphorus, and potassium fertility regimes affect tomato transplant growth. *HortScience*, *26*(2):141-142.

MOOY, L.M.; HASAN, A.; ONSILI.R. (2019) Growth and yield of Tomato (*Lycopersicum esculentum Mill*.) as influenced by the combination of liquid organic fertilizer concentration and branch pruning. IOP Conf. Series: *Earth and Environmental Science* 260(012170):1-8.

MORIARTY, C., COWLEY, D. C., WADE, T., & NICHOL, C. J. (2019). Deploying multispectral remote sensing for multi-temporal analysis of archaeological crop stress at Ravenshall, Fife, Scotland. *Archaeological Prospection*, 26(1): 33-46.

NICOLA, S.; BASOCCU, L. (1992). Nitrogen and N, P, K relation affect tomato seedling growth, yield and earliness. In *III International Symposium on Protected Cultivation in Mild Winter Climates 357*:95-102.

OLIVEIRA, T.F; PINTO, F.A.C; SILVA, D.J.H. (2019). Spectral Vegetation Indices applied to Nitrogen Sufficiency Index: A Strategy with Potential to Increase Nitrogen Use Efficiency in Tomato Crop. *Engenharia Agrícola* 39(1): 118-126.

PADILLA, F.M.; PEÑA-FLEITAS, M.T.; GALLARDO, M.; THOMPSON, R.B. (2015). Threshold values of canopy reflectance indices and chlorophyll meter readings for optimal nitrogen nutrition of tomato. *Annals of Applied Biology***,** 166: 271-285.

Parrot Drones, SA. (2017). Parrot Sequoia Technical Specifications. Retrieved January 28, 2019, from https://www.parrot.com/us/Business-solutions/parrot-sequoia#technicals

PALLOTTINO, F.; ANTONUCCI, F., COSTA C., BISAGLIA, C., FIGORILLI, S., & MENESATTI, P. (2019). Optoelectronic proximal sensing vehicle-mounted technologies in precision agriculture: A review. *Computers and Electronics in Agriculture*, *162*, 859-873.

PARTEL, V.; KAKARLA, S.C.; AMPATZIDIS,Y. (2019) Development and evaluation of a low-cost and smart technology for precision weed management utilizing artificial intelligence. *Computers and Electronics in Agriculture*, 157: 339-350.

PEDERSEN, S. M. LIND, K. M. (2017) Precision Agriculture–From Mapping to Site-Specific Application. In: *Precision agriculture: Technology and economic perspectives*. Springer, Cham, 77pp.

PINO, G.; PELUSO, A.M.; GUIDO, G. (2012). Determinants of regular and occasional consumers' intentions to buy organic food. *Journal of Consumer Affairs,* 46:157-169.

PREY, L.; von BLOH, M.; & SCGUMIDHALTER, U. (2018). Evaluating RGB imaging and multispectral active and hyperspectral passive sensing for assessing early plant vigor in winter wheat. *Sensors*, *18*(9): 2931-2949.

SHAMSHIRI et al., (2018), Research and development in agricultural robotics: A perspective of digital farming. *International Journal of Agricultural and Biological Engineering.*11(4):1-14

SINGH, K; KUMAR, S; KAUR, P. (2019) Automatic detection of rust disease of Lentil by machine learning system using microscopic images. *International Journal of Electrical and Computer Engineering (IJECE),* 9(1):660-666.

SOILLE, P. (2000). Morphological image analysis applied to crop field mapping. *Image and Vision computing*, *18*(13):1025-1032.

STAFFORD, J. (2019). *Precision agriculture for sustainability*. Burleigh Dodds Science Publishing Limited.

TARIQ, M.; SIDDIQI, AA.; NAREJO, G.B.; ANDLEEB, S. (2019). A Cross Sectional Study of Tumors Using Bio-medical Imaging Modalities. *Current Medical Imaging Reviews*, *15*(1): 66-73.

VAN EYSINGA, J. R.; SMILDE, K. W. (1981). *Nutritional disorders in glasshouse tomatoes, cucumbers and lettuce*. Centre for Agricultural Publishing and Documentation.

VELEY, K.; BERRY J.; FENTRESS S.; SCHACHTMAN, D.; BAXTER I; BART, R. (2017). High-throughput profiling and analysis of plant responses over time to abiotic stress*. Plant Direct* 1(4):e00023

VEYS, C. *et al*. (2019) Multispectral imaging for presymptomatic analysis of light leaf spot in oilseed rape. *Plant methods* 15(1): 1-12

WANG, Y. et al. (2019) Estimating soil nitrate leaching of nitrogen fertilizer from global meta-analysis. *Science of The Total Environment*, 657: 96-102

WILLER, H., SCHAAK, D., & LERNOUD, J. (2019). Organic farming and market development in Europe and the European Union. In *The World of Organic Agriculture. Statistics and Emerging Trends 2019* (pp. 217-254). Research Institute of Organic Agriculture FiBL and IFOAM-Organics International.

YOGAMALAGAN R, KARTHIKEYAN B. (2013).Segmentation techniques comparison in image processing*. International Journal of Engineering and Technology* 5:307-313

XUE, J.; FAN, Y.; SU, B.; FUENTES, S. (2019). Assessment of canopy vigor information from kiwifruit plants based on a digital surface model from unmanned aerial vehicle imagery. *International Journal of Agricultural and Biological Engineering*, *12*(1), 165-171.

XUE, J. and SU,B. (2017) Significant Remote Sensing Vegetation Indices: A Review of Developments and Applications. *Journal of Sensors* 2017:1-17.